LISBOA
SCHOOL OF
ECONOMICS &
MANAGEMENT

MASTER

MATHEMATICAL FINANCE

MASTER'S FINAL WORK

DISSERTATION

OPTION PRICING UNDER VARIABLE VOLATILITY

CATARINA NETO MARQUES

SEPTEMBER – 2017

LISBOA SCHOOL OF ECONOMICS & MANAGEMENT

MASTER

MATHEMATICAL FINANCE

MASTER'S FINAL WORK

DISSERTATION

OPTION PRICING UNDER VARIABLE VOLATILITY

CATARINA NETO MARQUES

SUPERVISIORS:

JOÃO PAULO VICENTE JANELA
ONOFRE ALVES SIMÕES

SEPTEMBER - 2017

Resumo

A teoria de valorização de opções que conhecemos hoje em dia deu o seu maior passo quando Fischer Black e Myron Scholes escreveram um artigo com uma fórmula fechada que permitia calcular os preços de opções Europeias de compra e venda cujo subjacente é uma acção ou um índice. No entanto, evidências mostram que a fórmula anterior não funciona bem num grande número de situações reais: os preços estimados desviam-se significativamente dos preços de mercado. Isto deve-se às hipóteses, muito restritivas, em que o modelo está assente.

Esta dissertação alarga o modelo de Black-Scholes a situações em que a volatilidade do preço do ativo é variável. As implicações desta extensão são estudadas tanto de um ponto de vista teórico como prático. Existem muitos modelos propostos para o caso em estudo e este trabalho foca-se nos modelos de volatilidade local porque mantêm as características mais importantes do modelo original. Foram selecionadas quatro funções diferentes para descrever a volatilidade do preço do ativo e um método de diferenças finitas foi implementado para obter estimações e previsões do preço de opções.

Os resultados obtidos realmente indicam que os modelos de volatilidade local estimam melhor os preços das opções do que o modelo de Black-Scholes original.

Palavras-chave: Valorização de opções, Volatilidade local, Método de Crank-Nicolson, Calibração.

Abstract

The modern theory of option pricing gave its biggest step when Fischer Black and Myron Scholes wrote a paper with a closed form solution for the prices of European call and put options on a single stock or index. However, evidence shows that the former formula no longer holds in many real cases: the estimated prices deviate significantly from the market ones. This is due to the very restrictive assumptions on which the model is based.

This dissertation extends the Black-Scholes model by making the volatility of the asset price variable. The implications of this extension are studied from both theoretical and practical points of view. Several models have been proposed and this work focuses on the local volatility models because they maintain the most important features of the classical model. Four different functions were selected to describe the volatility of the asset price and a finite difference method was implemented in order to obtain the estimations and predictions of the option prices.

The results suggest that indeed local volatility models have a better performance than the classical Black-Scholes model in estimating option prices.

Keywords: Option Pricing, Local Volatility, Crank-Nicolson scheme, Calibration.

Acknowledgments

First of all, I would like to thank my supervisors Prof. João Janela and Prof. Onofre Simões for their calm when I was stressed and letting me have the freedom in many of the decisions taken throughout the dissertation. To all the colleagues I met at ISEG and accompanied me during this important journey. Also, I would like to thank my parents and my brothers, who support me not only during my dissertation but during my whole life. A special thank you to my boyfriend, for the long afternoon sessions working on the dissertation and the encouragement words when I needed it.

Contents

Chapter 1

Introduction

Since 1973, when the famous paper by Black and Scholes appeared [1], a huge growth in the options market has been observed. These authors influenced the way investors saw this market and started the modern theory of option pricing. However, their model is based on assumptions that clearly do not match reality and evidence shows that the theoretical prices (prices predicted by Black-Scholes formula) deviate significantly from the market prices (prices at which options are actually traded). One of the most important assumptions of this model is that the stock price follows a geometric Brownian motion with constant volatility, which several authors showed not to be the case [5,8].

The aim of this dissertation is to build a model closer to reality by relaxing the constant volatility assumption and allowing for variable volatility in the asset price dynamics. This modification increases the complexity of the model, leading to a solution that cannot be obtained in a closed form. This drawback is counterbalanced by the fact that option prices closer to the market ones are expected to be obtained even if approximative methods are required.

Several alternatives have been proposed for the generalization of the Black-Scholes model and most of the literature is based on stochastic volatility [11, 12] and jump models [10], but we will focus on other type of models, called local volatility models [7, 9]. These models extend the classical Black-Scholes retaining its most important features without increasing the degree of uncertainty, in contrast with the former, which introduce non-traded sources of risk: stochastic volatility and jumps,

respectively. The local volatility models are characterized by a Partial Differential Equation (PDE) that explains the evolution of an option's price, which has the same form as the one obtained using classical assumptions. Nevertheless, it generally does not have an analytical solution, so it will be solved using numerical methods.

One of the most popular methods used in Finance in option problems when we have to solve a PDE is the Crank-Nicolson scheme [22], well suited for solving initial boundary value problems (IBVP). This scheme is second order accurate in time and space, gives good approximations for the solution and is relatively easy to program. Because of the nature of the chosen problem - a parametric local volatility model - calibration is needed in order to get the best possible fitting to the data (to implement the method and calibrate the model, we used MatLab code).

To compare the improved model to the standard Black-Scholes model, the prices for call options on the S&P 500 Index were estimated and set against the real market prices. Moreover, using the models that estimated the market prices better than the Black-Scholes, we tested their performance outside sample to see if the predictions were good.

The dissertation is structured as follows: Section 2.1 presents the classes of models found in the literature, concerning extensions of the Black-Scholes model, in particular the class of local volatility models. Section 2.2 contains the functions which will be used for the local volatility and in Section 2.3 the Partial differential equation for the price of an European option with underlying asset following a generalized Geometric Brownian Motion is derived. Chapter 3 is dedicated to the solution of the PDE presented in Section 2.3. In the first section of this chapter, we describe the numerical method used, the Crank-Nicolson method. Section 3.2 presents some PDEs usually found in Finance. The last section presents the calibration problem, which will allow for the choice of parameters in the functions described in Section 2.2. Chapter 4 describes the market data used and the results obtained. In the appendix, we can find the code used to implement the Crank-Nicolson scheme. We can also find the market data and the calibrated parameters for each of the models used.

Chapter 2

Option Valuation with Variable Volatility

Although Black and Scholes have influenced the modern theory of option pricing, the estimated prices using the original formula often quite diverge from the market ones, which led to several extensions of the classical model. One class of extensions is concerned with the assumption of constant volatility in the asset price dynamics, which is of the form

$$dS_t = \alpha S_t dt + \sigma S_t dWt,$$

where $\alpha \in \mathbb{R}$ is the mean return, $\sigma \in \mathbb{R}^+$ is the (local) volatility and W_t is a standard Wiener process. Using this model, a closed form solution for the price of an European call (or put) can be derived:

$$C(S,t) = N(d_1)S - Ke^{-r(T-t)}N(d_2), \tag{2.1}$$

where r is the risk-free rate, K is the strike price, T is the maturity and $d_1 = \frac{ln(S/K)+(r+\sigma^2/2)(T-t)}{\sigma\sqrt{T-t}}$ and $d_2 = d_1 - \sigma\sqrt{T-t}$.

Under the assumption of constant volatility, it is expected that, when inserting the market price of a call option into (2.1) with the respective strike and time to maturity, by solving it with respect to the volatility, the result is constant for different strikes and maturities. The volatility resulting from this process is called implied volatility.

The problem is that, by calculating the implied volatilities, we can observe a distinguish feature, usually denominated volatility smile: volatility depends both on strike and time to maturity [5, 8], contradicting the assumption of the Black-Scholes model. Generally, in stock and index options, it is observed what is called a negative skew: the implied volatility is a decreasing function of the strike price. The relationship of the implied volatility with time to maturity is called term structure and, in general, it is observed that the implied volatility increases with time to maturity. Using data from [18] of 77 call options on the S&P 500 Index and calculating the corresponding implied volatilities, we can observe the two features described in Figure 2.1:

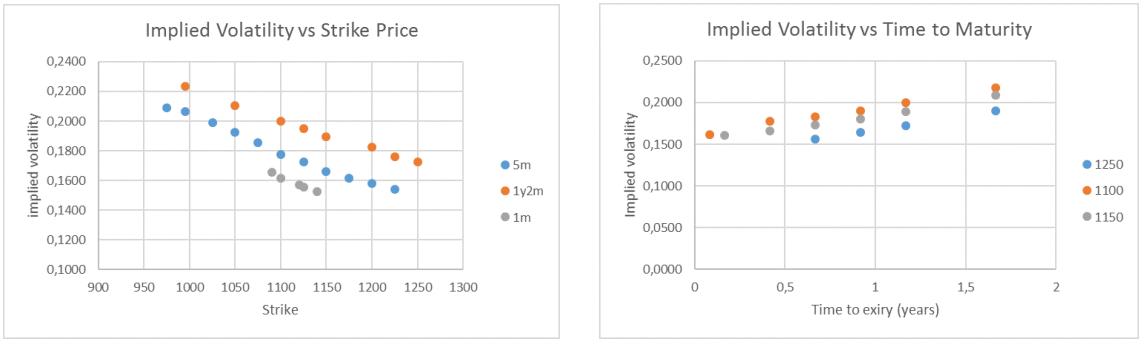

(a) Negative skew (b) Term structure

Figure 2.1: Properties of implied volatility

2.1 Extensions of the Black-Scholes Model

In the literature, there are essentially three different classes of extensions concerning the problem of variable volatility: stochastic volatility models, jump diffusion models and local volatility models. In this section, we will briefly discuss these alternative models, particularly the local volatility models.

In stochastic volatility models, as the name implies, the volatility of the asset is itself assumed to follow a stochastic differential equation, which frequently has some correlation with the stock price dynamics. This allows for skewness (measure of asymmetry) and leptokurtic (measure of tail weights) features in the distribution of the asset, which are many times observed in the market. The pioneers of this type of models were Hull and White [12], but there are several other authors that later used

this idea to account for the so-called volatility smile observable on option prices. Heston [11], for instance, used a mean-reverting equation to model the volatility and obtained a closed form solution for some types of options.

In jump diffusion models, the distribution of the underlying stock return is no longer continuous and the innovation is the introduction of a jump component in the asset dynamics, which allows for a positive probability of an abrupt change in the stock price. Merton [10] associates the appearance of a jump to outliers observed in stock series as a result of some announcement on the firm. This author highlights two different variations associated to the change in the stock price: the normal one, which follows Black-Scholes theory, and the abnormal variations, which arrive at discrete points in time and have the jump component. This results in a path for the stock price that is continuous most of the time, but sudden jumps of different sizes can occur. Finally, to obtain an equation that explains the evolution of the option price, Merton uses the Capital Asset Pricing Model (CAPM) and the fact that the jump component represents a non-systematic risk.

These two types of models have a common property: both of them add a new source of randomness (in the first case, the stochasticity of the volatility and in the second one, the jump component), which results in an incomplete market and a new approach must be made in order to find an equation for the option's price. We say that a market is complete if every financial derivative can be replicated; because the sources of uncertainty added in the first two models cannot be traded in the market, this replication is no longer possible and the completeness is lost (see [22] for a more precise cover of the topic).

The loss of completeness is not a problem for the local volatility models which stay close to the original Black-Scholes. The idea behind these kind of models is quite simple and intuitive: if the implied volatility depends on the strike and maturity of the option, then the local volatility depends on the price of the asset and on time. Then it can be assumed that the volatility of the asset is a deterministic function of the two variables, and we continue to have only one source of uncertainty: the Brownian motion in the asset's price dynamics. In the literature we can find, primarily, two different approaches: an implicit approach, where the volatility function $\sigma(S,t)$ is deduced from the smile, and a second approach, where the

volatility function assumes a specific form, i.e., an explicit expression is assumed. This specific function can be fixed or variable in the sense that it has some unknown parameters that are calibrated using market prices. The first kind of approach was initiated by Dupire [3], Derman and Kani [8] and Rubinstein [23], who used implied trees to extract the local volatility function from market data by matching the theoretical values of the options with the real ones. However, this exact fit to the current market data does not perform well when it is applied to predict future prices [4, 5]. Moreover, using this type of models does not give an intuitive explanation for the volatility function, contrarily to the second approach. Although the parametric local volatility approach, when calibrated with market data, also does not exactly match the option prices, it is the strategy chosen for this dissertation because it seems the best compromise between fitting market data and staying close to the classical BS model.

2.2 Local Volatility Functions

The work by Dumas, Fleming and Whaley [5] is one of the first attempts at explaining the local volatility function by giving a specific parametrization to $\sigma(S,t)$: these authors tried different quadratic models which resulted in a good fit when calibrating the parameters for the data used. Nevertheless, it didn't work outside the sample: the predicted prices were too different from the real ones. A number of other researchers contributed with answers to this problem, each one using a different approach, but always with the same goal in mind: to consider a local volatility function flexible enough to adjust to the market data (using calibration, for instance).

Following the work of Hull, Daglish and Suo [4] and Brown and Randall [6], the functions we have chosen to explain the local volatility of the asset are:

$$\begin{aligned}\sigma(S,t) = a_0 + a_1 ln(S/S_0) + a_2 ln(S/S_0)^2 + a_3(T-t) \\ + a_4(T-t)^2 + a_5 ln(S/S_0)(T-t)\end{aligned} \tag{2.2}$$

$$\sigma(S,t) = b_0 + b_1 \frac{ln(S/S_0)}{\sqrt{T-t}} + b_2 \left(\frac{ln(S/S_0)}{\sqrt{T-t}}\right)^2 + b_3 \left(\frac{ln(S/S_0)}{\sqrt{T-t}}\right)^3 \tag{2.3}$$

$$\sigma(S,t) = c_0 + c_1\frac{ln(S/S_0)}{(T-t)^{d_0}} + c_2\left(\frac{ln(S/S_0)}{(T-t)^{d_0}}\right)^2 + c_3\left(\frac{ln(S/S_0)}{(T-t)^{d_0}}\right)^3 \tag{2.4}$$

$$\begin{aligned}\sigma(S,t) = \sigma_{ATM}(t) + \sigma_{skew}(t)tanh\left(\gamma_{skew}(t)ln(S/S_0) - \theta_{skew}(t)\right)\\ \sigma_{smile}(t)\left(1 - sech\left(\gamma_{smile}(t)ln(S/S_0) - \theta_{smile}(t)\right)\right)\end{aligned} \tag{2.5}$$

Functions (2.2)-(2.4) are based on a set of rules of thumb proposed by investors and/or traders about the implied volatility surface. The authors [4] divide these rules in three classes: the strike rule, where the implied volatility is assumed to be independent of the asset price; the delta rule, where the implied volatility depends on the moneyness variable K/S; and the square root of time rule, where the implied volatility depends on time trough the square root of time left to maturity. Consulting the results found by the authors, we conclude that the first rule gives worse results compared to the other rules, so we do not insert any function concerning it.

In the last function (2.5), all functions σ, γ and θ are of the form $\frac{\beta_1+\beta_2 t}{1+\beta_3}$, with different parameters each. As the names appeal, σ_{ATM} describes the term structure of at-the-money volatilities, and the functions with *skew* and *smile* subscript account for the skew and smile components, respectively. Besides that, σ, γ and θ associated to these two components give the magnitude, width and centre, respectively, of the skew and smile. The functions chosen - hyperbolic tangent and hyperbolic secant - are based on the properties expected for the local volatility. The authors [6] state that, when pricing European options on stocks or indexes, making $\sigma_{smile}(t) = 0$ captures most of the behaviour and we do not need the extra parameters given by the last term on (2.5). Because a parsimonious model is preferable, when applying to market data, first we will use the model making the above adjustment and then, if the results are not as good as expected, the extra parameters will be added.

The parameters of the functions above are determined by calibration using available market data and we will study the estimation and prediction quality of the models by comparing the option prices that they supply with the real ones in and outside sample. This study will take place in Chapter 4 with a theoretical framework given in Chapter 3.

2.3 Generalized Black-Scholes Equation

The Black-Scholes model is based on a world where we have a non-dividend paying stock, denoted by S_t, and a risk-free asset, which will be denoted by B_t. Following [2], we will present a generalized Partial differential equation (PDE) where these assets can be characterized by the following dynamics:

$$\begin{aligned} dB_t &= rB_t dt \\ dS_t &= \alpha S_t dt + \sigma(S_t, t) S_t dWt \end{aligned} \tag{2.6}$$

where W_t is a standard Wiener process and the asset price follows a lognormal distribution with mean α and (local) volatility $\sigma(S, t)$. Also, r is the risk-free rate.

The only difference between the classical Black-Scholes and this generalized model is that the volatility of the stock price is non-constant, the remaining assumptions are maintained.

The derivation of the PDE consists in setting a riskless portfolio composed by a long position on an option and some amount on the respective underlying asset. This amount is chosen in such a way that the resulting portfolio is risk free or, in other terms, the dW_t term vanishes. Then, we will use the proposition below and the resulting PDE is easily obtained.

Proposition 1. *Suppose that there exists a portfolio such that the value process U has the dynamics*

$$dU = kUdt, \tag{2.7}$$

where k is a constant. Then, either $k = r$, or there exists an arbitrage possibility, where r is the same as in (2.6).

Let $V(t, S_t)$ be the price of an European option on the stock S_t at time t. The option and the stock are affected by the same source of uncertainty (movements in the stock price, in particular the Wiener process driving the stock's stochastic differential equation), so we can create a riskless portfolio consisting of a long position on the option and a short amount $\frac{\partial V}{\partial S}$ of the underlying stock. Let Π_t denote the

price of that portfolio at time t,

$$\Pi_t = V(t,S) - \frac{\partial V}{\partial S}S.$$

Using Itô's formula on $V(t,S)$, the infinitesimal change on the price of the portfolio is given by

$$d\Pi_t = \left(\frac{\partial V}{\partial t} + \frac{1}{2}\sigma(t,S)^2 S^2 \frac{\partial^2 V}{\partial S^2}\right) dt.$$

We can see that the choice of the amount of stock in the portfolio made the W_t term disappear from the portfolio's dynamics, eliminating the risk. This kind of manipulation is called delta hedging and must be performed continuously so that the portfolio is immune to changes in the stock price.

Without randomness in the portfolio, its dynamics must be equal to the one of the riskless asset or there will exist arbitrage opportunities, according to Proposition 1. Therefore, using (2.7), we have

$$\frac{\partial V}{\partial t} + \frac{1}{2}\sigma(t,S)^2 S^2 \frac{\partial^2 V}{\partial S^2} = r\left(V - \frac{\partial V}{\partial S}S\right).$$

Rearranging the terms, we get the equation,

$$\frac{\partial V}{\partial t}(t,S) + \frac{1}{2}\sigma(t,S)^2 S^2 \frac{\partial^2 V}{\partial S^2}(t,S) + rS\frac{\partial V}{\partial S}(t,S) - rV(t,S) = 0. \tag{2.8}$$

Equation (2.8) is the *Generalized Black-Scholes Partial Differential Equation*. In order to get the full problem we need to add extra conditions that will depend on the type of option to be priced, i.e, if it is a call or a put option.

Even though it seems that this PDE is not that different from the one found on [1], in general, it has no closed form solution, so it needs to be solved numerically as we will see in the next chapter.

Chapter 3

Numerical Methods for Option Pricing

When the option pricing models become more complex, it has been discussed that it is no longer possible to obtain analytical solutions and numerical ones have to be found. In the literature, there are three classes of methods that often appear: tree-based methods, Monte Carlo method and finite difference methods [16, 22, 24].

Tree-based methods rely on the assumption that the stock price, in the next time step, will have a known number of possible values with given probabilities (in the case of binomial trees we have two possibilities, trinomial trees display three possibilities, etc.); then a tree of these stock prices is build until the maturity of the option. At the maturity, the value of the option is known and, from there, at each node of the tree, the price of the option is calculated backwards by discounting the expected value of the option prices in the nodes ahead.

Monte Carlo is a simulation method. It repeatedly generates sample paths of the underlying, assuming a lognormal distribution for the asset price. This generation is done until expiry, where we can have an estimated value for the option. Then, we take the average of all the estimations for the option price and discount it back to the present.

Finite Difference methods are applied when one needs to solve numerically a Partial differential equation. These methods convert the PDE into a system of linear equations by replacing the derivatives with the respective finite difference

approximations.

Monte Carlo method converges slowly (we may need to run it many times until we get a good approximation, resulting in a high computational cost), which makes it an undesirable choice. However, when we have an option based on more than two assets, it becomes more efficient [24, 25] and is widely used in such cases. Although simple and easy to implement, tree methods also converge at a slow rate. Finite Difference methods are efficient when dealing with options based on a single asset [24], which is a plus comparing with the former methods. Moreover, it is easy to program and handles well coefficients that are time and/or space dependent as in (2.8). The advantages provided by this method are the reason why it will be the one used to estimate the option prices in Chapter 4.

The problem one wants to solve is the following:

Find a function $u(x,t) : D \to \mathbb{R}$, with $D = [A,B] \times [0,T]$ satisfying:

$$-\frac{\partial u}{\partial t} + a(x,t)\frac{\partial^2 u}{\partial x^2} + b(x,t)\frac{\partial u}{\partial x} + c(x,t)u = f(x,t) \; in \; intD \tag{3.1}$$

$$u(x,0) = u_0(x), \; x \in [A,B] \tag{3.2}$$

$$u(A,t) = g_0(t), \; u(B,t) = g_1(t), \; t \in [0,T] \tag{3.3}$$

This type of problem is usually called a reaction-advection-diffusion problem. Functions $a(x,t)$, $b(x,t)$ and $c(x,t)$ are associated to diffusion, advection and reaction coefficients, respectively. It has an initial condition and Dirichlet boundary conditions.

3.1 Finite Difference Methods Overview

The first step when dealing with finite difference methods is to discretize the domain both in time and space, resulting in a uniform grid:

- In time: divide $[0,T]$ into N equally spaced intervals $0 = t_0 < t_1 < ... < t_N = T$, with length $k = \frac{T}{N}$, resulting in $N+1$ points, denoted by $t_i = ik, \; i = 0, ...N$;
- In space: divide $[A,B]$ into M equally spaced intervals $A = x_0 < x_1 < ... < x_N = B$, with length $h = \frac{B-A}{M}$, resulting in $M+1$ points, denoted by

$$x_j = A + jh,\ j = 0, ..., M.$$

A generic node at the grid is identified by the indices i and j as (t_i, x_j). This discretization results in a grid with $(N+1) \times (M+1)$ points as in Figure 3.1. The aim of this method is to approximate the function $u(x,t)$ at these grid-points.

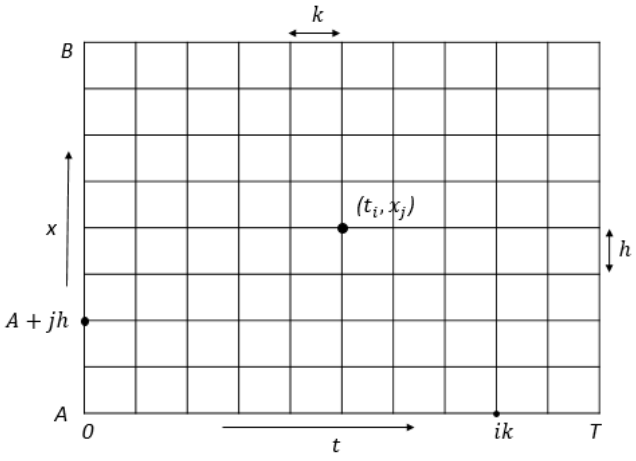

Figure 3.1: Space-time discretization

There are three classic finite difference methods usually applied to IBVPs such as (3.1)-(3.3): Euler explicit scheme, Euler implicit scheme and Crank-Nicolson scheme. The explicit scheme is the simplest one, but it has the disadvantage of being conditionally stable, that is, its stability depends on h and k and their relationship, more precisely, k/h^2 must be less than a certain constant. Using this scheme, for each time step, we obtain explicitly the value of a grid-point (x_i, t_{j+1}) using three values of the previous time step: (x_{i-1}, t_j), (x_i, t_j) and (x_{i+1}, t_j).

If a scheme is not stable, the numerical error tends to accumulate as we go further in time and we cannot guarantee that it remains bounded. This problem is handled using implicit schemes. The implicit Euler method is unconditionally stable and the value of a grid-point (x_i, t_j) is obtained using three values of the next time step: (x_{i-1}, t_{j+1}), (x_i, t_{j+1}) and (x_{i+1}, t_{j+1}). Here, an explicitly relation cannot be achieved and a linear system of equations needs to be solved at each time step.

Finally, the Crank-Nicolson scheme is an average of the two previous schemes and has the advantage of being second order accurate in both the x and t directions, while the other schemes are second order accurate in the x direction but only first

order in the t direction [13]. Hence, Crank-Nicolson method is the most precise of the three and this is the reason why is the one used in the dissertation.

As already mentioned, in this methods we deal with differences instead of derivatives. By Taylor's expansion, we can write to some function $\phi(x,t)$:

$$\phi(x \pm h, t) = \phi(x,t) \pm h\frac{\partial \phi}{\partial x}(x,t) + \frac{h^2}{2}\frac{\partial^2 \phi}{\partial x^2}(x,t) \pm \frac{h^3}{6}\frac{\partial^3 \phi}{\partial x^3}(\eta_{\pm}, t)$$
$$\phi(x, t+k) = \phi(x,t) + k\frac{\partial \phi}{\partial t}(x,t) + \frac{k^2}{2}\frac{\partial^2 \phi}{\partial t^2}(x,\upsilon)$$

with $\eta_+ \in (x, x+h)$, $\eta_- \in (x-h, x)$ and $\upsilon \in (t, t+k)$.

Rearranging the terms, we get the following:

$$D_+\phi(x,t) \equiv \frac{\phi(x,t+k) - \phi(x,t)}{k} = \frac{\partial \phi}{\partial t}(x,t) + \mathcal{O}(k) \tag{3.4}$$
$$D_+D_-\phi(x,t) \equiv \frac{\phi(x+h,t) - 2\phi(x,t) + \phi(x-h,t)}{h^2} = \frac{\partial^2 \phi}{\partial x^2}(x,t) + \mathcal{O}(h^2) \tag{3.5}$$
$$D_0\phi(x,t) \equiv \frac{\phi(x+h,t) - \phi(x-h,t)}{2h} = \frac{\partial \phi}{\partial x}(x,t) + \mathcal{O}(h^2) \tag{3.6}$$

(3.4) is called a *forward difference approximation* and is a first order approximation to the first derivative of ϕ with respect to (w.r.t.) t. (3.6) is called a *centre difference approximation* and is a second order approximation to the first derivative of ϕ w.r.t. x. Finally, (3.5) is a second order approximation to the second derivative of ϕ w.r.t. x.

Then, we have the following approximations of the derivatives in (3.1):

$$\frac{\partial \phi}{\partial t}(x,t) \approx \frac{\phi(x,t+k) - \phi(x,t)}{k}$$
$$\frac{\partial^2 \phi}{\partial x^2}(x,t) \approx \frac{\phi(x+h,t) - 2\phi(x,t) + \phi(x-h,t)}{h^2}$$
$$\frac{\partial \phi}{\partial x}(x,t) \approx \frac{\phi(x+h,t) - \phi(x-h,t)}{2h},$$

which can provide approximate values for $\frac{\partial \phi}{\partial t}$, $\frac{\partial^2 \phi}{\partial x^2}$ and $\frac{\partial \phi}{\partial x}$ at any grid point, given the values of ϕ.

3.1.1 Crank-Nicolson method

At this point, the goal is to convert the continuous problem (3.1)-(3.3) to the corresponding discrete version based on the Crank-Nicolson method. We begin by enumerating some properties of this scheme:

- *Consistency*: It is consistent. This means that the finite difference representation converges to the PDE as h and k tend to zero;
- *Stability*: It is unconditionally stable with respect to h and k, i.e., for any choice of these two steps, the error remains bounded;
- *Convergence*: It is convergent, i.e, the numerical solution tends to the exact solution when $N, M \to \infty$;
- *Accuracy*: It has a second order accuracy with respect to both x and t, i.e., $|\tau_j^i| \leq C(h^2 + k^2)$, where C is a constant and τ_j^i is the truncation error (see [13]). The order in x comes directly from (3.5) and (3.6); because this scheme is evaluated at $\frac{1}{2}(t_i + t_{i+1})$, using a centre difference approximation to the first derivative of u w.r.t t, we get an order of two in time as well.

The notation in this section follows Duffy [14]. Let L_h^k be the discrete operator defined at the grid-points. One wants to approximate the function $u(x,t) : D \to \mathbb{R}$, with $D = [A,B] \times [0,T]$ at the grid-points, that is, to find $u_j^i = u(x_j, t_i)$ such that:

$$-\frac{u_j^{i+1} - u_j^i}{k} + \frac{1}{2}(L_h^k u_j^i + L_h^k u_j^{i+1}) = f_j^{i+1/2},\ i = 1, ..., N-1,\ j = 1, ..., M-1 \quad (3.7)$$

$$u_j^0 = u_0(x_j),\ j = 0, ..., M \quad (3.8)$$

$$u_0^i = g_0(t_i),\ u_M^i = g_1(t_i),\ i = 1, ..., N\ , \quad (3.9)$$

where $L_h^k u_j^i = a_j^i D_+ D_- u_j^i + b_j^i D_0 u_j^i + c_j^i u_j^i$, $a_j^i = a(x_j, t_i)$, $b_j^i = b(x_j, t_i)$, $c_j^i = c(x_j, t_i)$, $f_j^i = f(x_j, t_i)$, with functions a, b, c and f the same as in (3.1) and

$$D_+ D_- u_j^i = \frac{u_{j+1}^i - 2u_j^i + u_{j-1}^i}{h^2},$$
$$D_0 u_j^i = \frac{u_{j+1}^i - u_{j-1}^i}{2h}.$$

The system (3.7)-(3.9) does not give an intuitive idea of how we can get the values of u at the grid-points, but we can transform it into a system of linear equations. Expanding (3.7), we get

$$-\frac{u_j^{i+1}-u_j^i}{k}+\frac{1}{2}\left(a_j^i\frac{u_{j+1}^i-2u_j^i+u_{j-1}^i}{h^2}+b_j^i\frac{u_{j+1}^i-u_{j-1}^i}{2h}+c_j^iu_j^i\right)$$
$$+\frac{1}{2}\left(a_j^{i+1}\frac{u_{j+1}^{i+1}-2u_j^{i+1}+u_{j-1}^{i+1}}{h^2}+b_j^{i+1}\frac{u_{j+1}^{i+1}-u_{j-1}^{i+1}}{2h}+c_j^{i+1}u_j^{i+1}\right)=f_j^{i+1/2}.$$

Rearranging the terms and multiplying by $4h^2k$, it follows

$$A_iu_{j+1}^{i+1}+B_iu_j^{i+1}+C_iu_{j-1}^{i+1}=D_i\ ,$$

where $A_i=2ka_j^{i+1}+hkb_j^{i+1}$, $B_i=-4h^2-4ka_j^{i+1}+2h^2kc_j^{i+1}$, $C_i=2ka_j^{i+1}-hkb_j^{i+1}$ and $D_i=-[u_{j+1}^i(2ka_j^i+hkb_j^i)+u_j^i(4h^2-4ka_j^i+2h^2c_j^i)+u_{j-1}^i(2ka_j^i-hkb_j^i)]+4h^2kf_j^{i+1/2}$, for $i\in\{1,...N\}$ *and* $j\in\{1,...,M\}$.

Specifically, starting with a given initial condition, we obtain the solution at the next time step by solving the following linear system:

$$\begin{bmatrix}1&0&0&\dots&\dots&0\\C_1&B_1&A_1&0&\dots&0\\0&C_2&B_2&A_2&\dots&0\\0&0&\ddots&\ddots&\ddots&0\\0&\dots&0&C_{M-1}&B_{M-1}&A_{M-1}\\0&0&0&\dots&0&1\end{bmatrix}\begin{bmatrix}u_0^{i+1}\\u_1^{i+1}\\u_2^{i+1}\\\vdots\\u_{M-1}^{i+1}\\u_M^{i+1}\end{bmatrix}=\begin{bmatrix}D_0\\D_1\\D_2\\\vdots\\D_{M-1}\\D_M\end{bmatrix}$$

The matrix on the left side is a $(M+1)\times(M+1)$ matrix and D_0 and D_M are the boundary conditions at $x=A$ and $x=B$, respectively.

To implement the Crank-Nicolson method we used MatLab. The code for the general system of equations (3.1)-(3.3) can be found in A1.

3.2 Important PDEs Found in Finance

This overview of some numerical methods had the goal of solving Equation (2.8). This equation needs complementary conditions in order to have a unique solution.

In the case of European vanilla call and put options, denoting the price of the put by $P(S,t)$, we have the conditions:

$$C(S,T) = max(S-K,0)\ , P(S,T) = max(K-S,0) \tag{3.10}$$

$$C(0,t) = 0\ , P(0,t) = Ke^{-r(T-t)} \tag{3.11}$$

$$C(S,t) \to S - Ke^{-r(T-t)},\ P(S,t) \to 0\ as\ S \to \infty \tag{3.12}$$

Comparing (2.8) plus the complementary conditions (3.10)-(3.12) with problem (3.1)-(3.3), there are two differences: the first is the fact that, in the option problem, we have a terminal condition while in the generalized problem we have an initial condition; the second is that, in the option problem, the domain of the variable S is infinite and in the generalized problem the domain is bounded. So, one needs to make some adjustments in the options problem in order to solve it using C-N method: truncate the domain of S and perform a change of variables so that t denotes time left to maturity and not maturity itself.

Artificially truncating the domain of the asset price implies an additional error to the finite difference scheme. To attenuate the effect of this error, one must choose the maximum value of the asset price - let S_{max} be that value - far enough of the so called region of interest, but not too far as to bring a lot of computer effort. Investigations from [20] and [21] suggest a value of about three to four times the highest strike of the market data available.

In the next subsections, three examples of Partial differential equations commonly found in Finance are given. These PDEs are going to be used to get the estimated prices of options that we then use to compare with the market prices. The choice of the PDE we will use to estimate the prices will depend on the type of data used.

Forward PDE

In this first adjustment, we will truncate the domain in the variable S as $[0, S_{max}]$. The following change of variable is done: $t^* = T - t$, where t^* stands for time left to maturity, that is, we have now a function $V^*(S,t^*) = V(S,T-t^*)$. Therefore, we

have

$$\frac{\partial V^*}{\partial t^*} = \frac{\partial V}{\partial t}\frac{\partial t}{\partial t^*} = -\frac{\partial V}{\partial t}.$$

Replacing this derivative in (2.8) and returning to the original variable names, i.e., t and $V(S,t)$ denoting time to maturity and price of the option, respectively, we get the new PDE (with respective conditions) in the call case:

$$\begin{aligned}
&-\frac{\partial V}{\partial t} + \frac{1}{2}\sigma(t,S)^2 S^2 \frac{\partial^2 V}{\partial S^2} + rS\frac{\partial V}{\partial S} - rV = 0,\ t \in (0,T)\ , S \in (0, S_{max}) \\
&V(S,0) = max(S-K,0) \\
&V(0,t) = 0,\ V(S_{max},t) = S - Ke^{-rt}
\end{aligned}$$

This is called a *forward Partial Differential Equation.*

Logarithmic PDE

In this second adjustment, we will perform two changes of variables: $t^* = T - t$ and $x = log(S)$. The first one is exactly the same as above, the second transforms the prices into its logarithm. Now, the resulting function is $V'(x,t^*) = V(e^x, T-t^*)$ and we calculate the derivatives:

$$\begin{aligned}
\frac{\partial V'}{\partial t^*} &= \frac{\partial V}{\partial t}\frac{\partial t}{\partial t^*} = -\frac{\partial V}{\partial t} \\
\frac{\partial V'}{\partial x} &= \frac{\partial V}{\partial S}\frac{\partial S}{\partial x} = S\frac{\partial V}{\partial S} \\
\frac{\partial^2 V'}{\partial x^2} &= S\frac{\partial V}{\partial S} + S\frac{\partial^2 V}{\partial S^2}\frac{\partial S}{\partial x} = S\frac{\partial V}{\partial S} + S^2\frac{\partial^2 V}{\partial S^2}.
\end{aligned}$$

In this case, the domain of the variable x is truncated as (x_{min}, x_{max}), where x_{min} no longer needs to be zero. Now, again denoting t as time left to maturity, we can write the PDE (with respective conditions) for a call option:

$$\begin{aligned}
&-\frac{\partial V}{\partial t} + \frac{1}{2}\sigma(x,t)^2\frac{\partial^2 V}{\partial x^2} + \left(r - \frac{1}{2}\sigma(x,t)^2\right)\frac{\partial V}{\partial x} - rV = 0,\ t \in (0,T)\ , x \in (x_{min}, x_{max}) \\
&V(x,0) = max(e^x - K, 0) \\
&V(x_{min},t) = 0,\ V(x_{max},t) = e^x - Ke^{-rt}
\end{aligned}$$

According to [13], when pricing vanilla options, the choice between these two PDEs does not affect the solution in a significant way, what really matters is to use a suitable grid.

Dupire PDE

Here, we are going to present a particular Partial Differential Equation for a call option as a function of strike and time to maturity, $C(K,T)$, derived by Dupire, see [13]. Fixing $t = 0$ and denoting the spot price by S_0, the price of a call option must satisfy the following PDE:

$$
\begin{aligned}
&-\frac{\partial C}{\partial T} + \frac{1}{2}\sigma(K,T)^2K^2\frac{\partial^2 C}{\partial K^2} - rK\frac{\partial C}{\partial K} = 0,\ T \in (0, T_{max})\ , K \in (0, K_{max}) \\
&C(K,0) = max(S_0 - K, 0) \\
&C(0,T) = S_0,\ C(K_{max}, T) = 0
\end{aligned}
$$

This equation is called *Dupire PDE* and allows to price call options with various strikes and maturities on the same underlying asset.

Comparing the three Partial Differential Equations above with problem (3.1)-(3.3), the generic coefficient and respective conditions become:

	Forward PDE	**Logarithmic PDE**	**Dupire PDE**
$a(x,t)$	$\frac{1}{2}\sigma(S,t)^2S^2$	$\frac{1}{2}\sigma(x,t)^2$	$\frac{1}{2}\sigma(K,T)^2K^2$
$b(x,t)$	rS	$r - \frac{1}{2}\sigma(x,t)^2$	$-rK$
$c(x,t)$	$-r$	$-r$	0
$f(x,t)$	0	0	0
$u_0(x)$	$max(S-K,0)$	$max(e^x - K, 0)$	$max(S_0 - K, 0)$
$g_0(t)$	0	0	S_0
$g_1(t)$	$S - Ke^{-rt}$	$e^x - Ke^{-rt}$	0

Table 3.1: PDEs found in Finance

3.3 Calibration

Model calibration can be defined as the process of fitting models to market data. These models can depend on some unknown parameters (as the local volatility functions chosen in Section 2.2) which will be calibrated using observations taken

from the market. The aim is to choose the parameters in such a way that the estimated prices are as close as possible to the market prices. The term close has no unique definition, it will depend on the problem formulated, particularly, on the function chosen to minimize the differences.

In general, the first step when one wants to calibrate a model is to choose which function (generally called objective function) will be minimized and, once this decision is made, choose which optimization process will be used to minimize the objective function.

One way to solve the calibration problem is via least squares formulation. Least squares are broadly discussed in the literature [22] in its linear form, but the structure of our problem excludes this possibility, so we have to work with nonlinear least squares. Even though this form can fit a wide range of functions, it has the following disadvantage: an iterative algorithm needs to be used in order to get the parameter estimates. Besides the fact that the implementation is harder than in the linear case (where the solution can be found analytically), this kind of methods are not flawless, that is, they strongly depend on the initial solution, and more than one stopping condition must be imposed so that the algorithm terminates, even if an optimum is not reached. Nevertheless, theory behind non linear least squares is well developed [26] and MatLab has an incorporated function which handles this kind of problems. From now on, we will only talk about nonlinear least squares. The procedure consists in finding the best fitting to a given set of points by minimizing the sum of squares of the offsets of the points from the fitted values, i.e., find the coefficient $a \in \mathbb{R}^p$ which solves the problem of finding:

$$arg \min_a \sum_{i=1}^{n} [y_i(a) - ydata_i]^2$$

This method can be extended so it handles restrictions on the search domain for $a = (a_1, ..., a_p)$.

The MatLab function to solve such problems works, summarily, in this way [29]:

1. Starts with an initial estimate for each coefficient, called initial solution;

2. Calculates the value of the objective function for the current set of coefficients;

3. Adjusts the coefficients and determines whether the fit improves. The function has five different algorithm choices and the default one can solve most of the problems, so that's the one which will be used;

4. Iterate the process by returning to step 2 until the fit reaches the specific convergence criteria. The convergence criteria has four types of situations: function converges to a solution; change in the solution is less than a certain value; change in the residual is less than a certain value; or magnitude of search direction is smaller than a pre-established value.

For the choice of initial solution in step 1, if we do not have any prior information that could give us an intuition about it, we should generate many sets of initial values and select the one that leads to a better solution (in our case, the solution which has the lowest value).

Local Volatility Model

In our particular case, i.e., in the local volatility model, is quite straightforward that each choice of parameters for $\sigma(t, S)$, fixing one of the functions (2.2)-(2.5), gives a different solution to the option value, so one needs to estimate the parameters that give the minimum value for the sum of the squared differences between the estimated price and the observable one. Our problem is of the type:

$$arg \min_{a \in \mathbb{R}^p} \sum_{i=1}^{n} [V(K_i, T_i; a) - V_i^*]^2 \tag{3.13}$$

$$s.t.\ \sigma(t, S; a) \geq 0 \tag{3.14}$$

where n is the number of market observations, V is the price estimated by the model with strike K_i, maturity T_i, and volatility parameter a, and V^* is the market value for the same strike and maturity. The data used in this problem consists of a family of vanilla call or put options with different strikes and maturities on some underlying asset (stock or index).

Chapter 4

Results

To get the results searched for this dissertation, one needs to do the following: for each local volatility function defined in Chapter 2, calculate the estimated prices for a call or put option using the Crank-Nicolson scheme, choosing one of the PDEs in Section 3.3. This method will return a grid where each point defines an option price for a given maturity and strike.

The grid constructed is uniform (see Figure 3.1), so the prices of the options produced by the Crank-Nicolson method will have strikes and times left to maturity evenly spaced. The probability of getting option data which lies in these exact points is low, so we need to find a way to deal with this problem. It can be overcome by using interpolation between the values calculated at the grid points: according to [20] and [21] a cubic spline interpolation should be sufficient as it will not affect the error in a significant way.

After interpolating the estimated data, we are ready for the calibration by just using the MatLab function to minimize the sum of the squared differences between the interpolated data and the market one, subject to the constrain that the local volatility must be non-negative (problem (3.13)-(3.14)). Once we have all the parameters for each local volatility function, we can compare the results to see which model(s) seems more suitable and if it is really an improvement over the standard Black-Scholes. Besides that, we should also see if the qualitative properties showed in Figure 2.1 for the local volatility are preserved.

From the beginning of this work, it is clear that the only difference between the

local volatility model and the standard Black-Scholes model is the assumption of constant volatility. This modification is made in order to get closer to reality and hence to improve the capacity of estimation of the BS model; therefore, throughout the next sections, we will start by giving the results using the standard Black-Scholes model and then will use these values to assess the quality of the new models.

4.1 Data

The market data used in this dissertation consists of call options whose underlying is the S&P 500 Index. This decision was made based on the amount of options traded daily on this Index and, since more trades give a better perspective of the market, we chose one of the most active options in the market. From the various strikes and maturities available, 86 options were chosen with strike prices varying from 2150$ to 2650$ and time left to maturity from 8 days to 638 days (March 2017 to December 2018). These options were taken on 23 March 2017 and at the close of the market the S&P 500 Index was worth 2345.96$. It is a common practice to work with midprices (see [22] for instance), that is, the average between the bid (maximum price that a buyer is willing to pay) and ask (minimum price that a seller is willing to receive) prices:

$$C_i = \frac{C_i^{ask} + C_i^{bid}}{2}.$$

The midprices for the 86 call options and a plot of the prices against strike can be found in Appendix A.2.

Both the Forward PDE and the Logarithmic PDE presented in Section 3.2 are used to obtain the price of an option where the strike is fixed and the asset price is variable. Since our data consists of points of the form (K_i,T_i), where K_i is the strike and T_i is the time left to maturity of the ith option, respectively, it seems that the Dupire PDE is the most suitable choice, because it treats the call option as a function of both strike and time left to maturity.

To get all the data for the calculation of the option prices, we still need one more element: the risk-free rate. This value is defined as the return of an investment with no risk, but in real life such thing does not exist because every investment carries

some risk, even if it is insignificant. Frequently, government security rates are used as a proxy for risk-free rates, either short-term or long-term [27]. In practice, it is common to use the interest rate on a three-month U.S. Treasury Bill as a proxy for the risk-free rate, and we will follow it. From the U.S. Department of the Treasury [28] was possible to recover the T-Bill rates on 23 March 2017. In Table 4.1, we can observe the values for different time horizons.

4 Weeks	**13 Weeks**	**26 Weeks**	**52 Weeks**
0.72	0.75	0.88	0.95

Table 4.1: Treasury Bill Rates on 23 March 2017 (%)

Reading the table and taking into account the usual practice, we obtain a risk-free rate of 0.75% (75 basis points).

4.2 Parameter Calibration and Estimation

In the next sections we will present the results of the calibration of the standard Black-Scholes model and the local volatility model, using the dataset described in the previous section. All four functions for the volatility are used, so we will end with four different estimations plus the Black-Scholes estimation for the option prices.

The comparison between the different models and the market prices will have two components: a "numerical" one, using different measures to describe the goodness of the fit, and a "visual" one, where we plot the market prices against the model ones. In this plot, the market prices are denoted by a blue circle and the model prices by a red plus sign. The goal is to calibrate the models in such a way that the plus signs and the circles overlap or stay as close as possible.

4.2.1 Black-Scholes model

Using the Black-Scholes formula for call options (2.1) to estimate the option prices and stating the volatility parameter σ as the unknown parameter which needs to be calibrated, we get a value of $\sigma = 11.79\%$. This is the value which gives the best fit by minimizing the squared differences between the BS prices and the market ones and we can see in Figure 4.1 the comparison between them.

Although for the shorter maturities the estimation is accurate, we observe that, as the maturity increases, there is a big discrepancy between the estimated and the market prices. This evidence is expected and backs up what was mentioned on the introduction regarding the quality of the BS model in market price estimation.

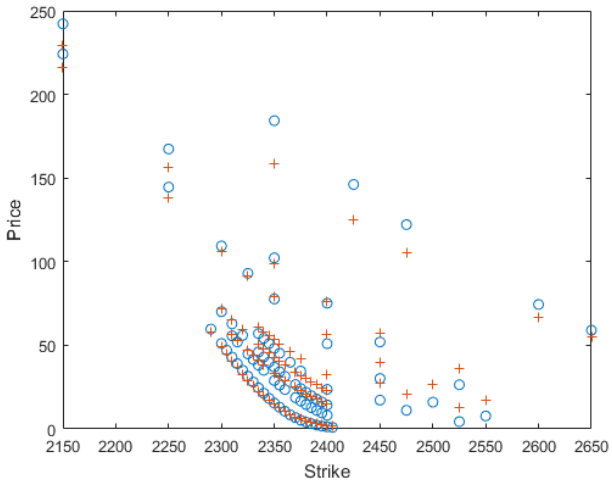

Figure 4.1: Market Prices *vs.* Black Scholes estimation

4.2.2 Local Volatility model

At this point, we will make a parameter calibration using the four different local volatility functions (2.2)-(2.5). The variable t is defined in years and varies from 0 to 2.5 to include all the maturities of the data. The variable K varies from 0 to 8000.

Using the procedure already described at the beginning of this chapter, we made some experiments using different steps (time and space) on the Crank-Nicolson method and different starting points for the minimization of the objective function. Changing the time and space steps of the scheme does not change the magnitude of the results, that is, it increases or decreases the value of the objective function but not in a significant way. The running time of the program (computational time) didn't change much using bigger or smaller steps, so we decided to use $M = 400$ and $N = 100$, with M and N having the same notation as in Chapter 3. The same cannot be said about the starting points: in all models, except Model 1, a different starting point can give a different solution. To try to overcome this problem, we

started at different starting points and kept the solution which gave the lowest value for the objective function. This behaviour can be associated to the existence of local minimum points.

For the first function (2.2), we can find the value of the calibrated parameters in Table A.2 in the Appendix. Looking at Figure 4.2 (a), we can see that there exists a big improvement over the Black-Scholes model as the estimated prices are closer to the real ones, particularly at longer maturities, which were the ones where the Black-Scholes estimation was less accurate. For almost all the prices the crosses are inside the circles, i.e, there exists an overlap between estimated and real prices, which is the aim when one uses a model to describe the options market.

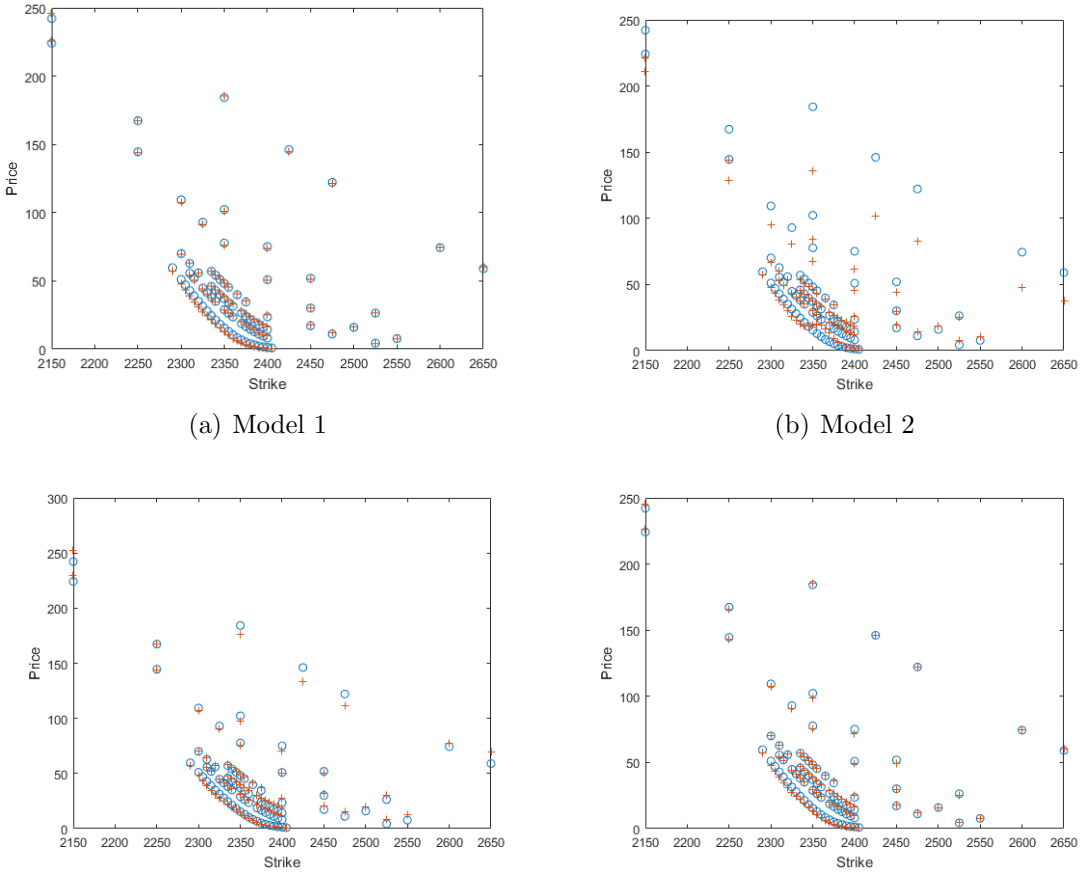

(a) Model 1

(b) Model 2

(c) Model 3

(d) Model 4

Figure 4.2: Market prices *vs.* model estimations

For the second function (2.3) the same didn't happen. The estimated prices are even further from the real ones when we compare them to the BS estimation. This difference is more notable when we look at the longer maturities as we can see in

Figure 4.2 (b), which is where this models seems to fail more. The parameters values can be found in the Appendix, Table A.3.

The third function (2.4) is an extension of the previous one. The only difference is an extra parameter which gives more flexibility, hence we expect this model to give better results than the second. This is indeed true, there exists an improvement over Model 2 and even more, this improvement extends to the BS model. Comparing Figure 4.2 (c) and Figure 4.1, we can see that the prices estimated by this model are closer to the real ones. Nevertheless, there are still some prices that are far from the market ones. The parameters can be found in Table A.4.

The fourth function (2.5) produces Figure 4.2 (d), where we can observe an improvement over the Black-Scholes estimation. It seems that this model had a better performance than the third in estimating the option prices (particularly at longer maturities) and the results are similar to the ones produced by Model 1. The parameters can be found in Table A.5.

With the parameters obtained from the calibration, we can construct the local volatility surface for each function. Figure 4.3 shows the local volatility as a function of time left to maturity and asset price and its values are in percentage.

The local volatility surface generated by Model 1 in Figure 4.3 (a) shows, in overall, the properties expected for the local volatility: as the asset price decreases its value increases and increases as the maturity rises. For the longest maturity, there is an exception: the volatility decreases a little before it starts increasing. Observing Figure 4.3 (b), we can see that for the second model the volatility is practically plain in the domain under consideration. This means that, even considering a deterministic function for the volatility, when we calibrate the parameters, the volatility becomes constant, in this case, with a value around 10%. For the third model, the relationship of the volatility with maturity follows the expected pattern, i.e., it increases as the maturity increases. For the relationship with the asset price, the shape is not what we excepted, instead it is a U-shape. Finally, observing Figure 4.3 (d) we can see that Model 4 shows, in overall, the features we expected, with one exception. For small values of the asset price, the volatility decreases when the maturity increases, which contradicts the properties seen in Figure 2.1.

From Figure 4.2, we can conclude, at a first glance, that the second model is not

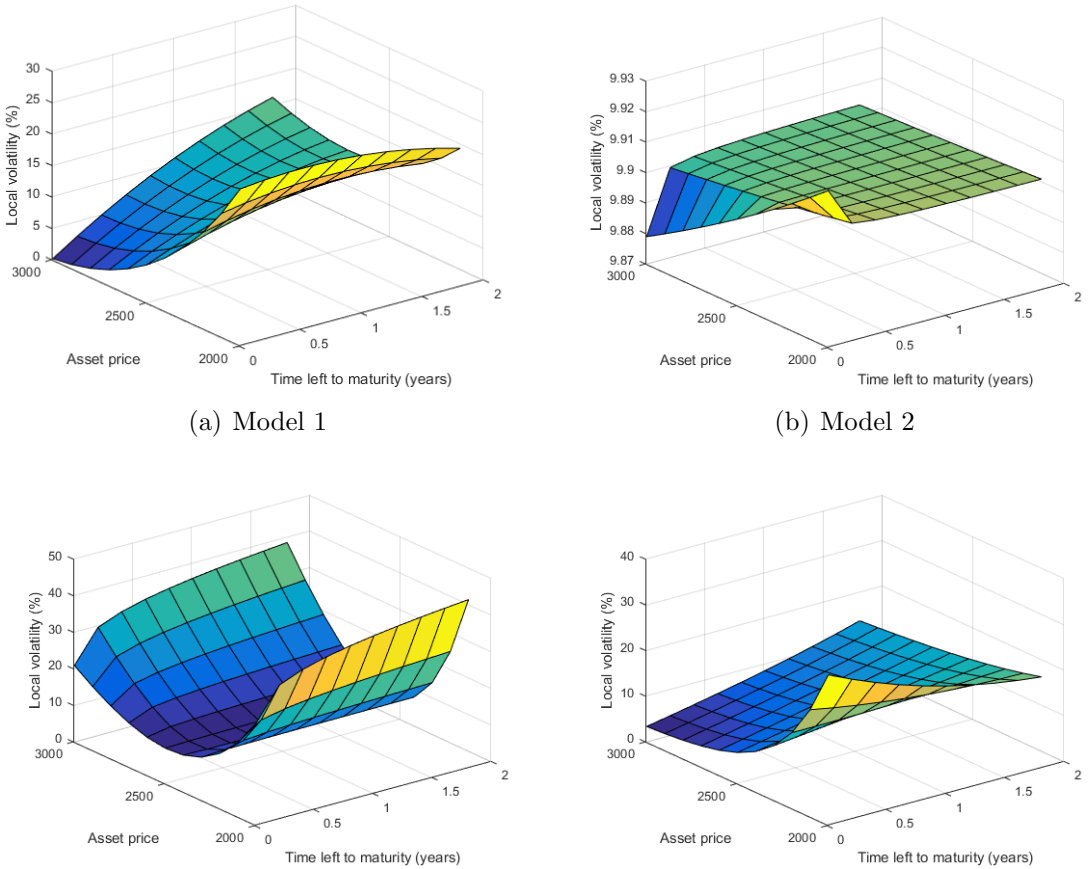

(a) Model 1

(b) Model 2

(c) Model 3

(d) Model 4

Figure 4.3: Local volatility surface for each model

better than Black-Scholes in estimating the option prices. As for models 1, 3 and 4, we saw a substantial improvement as they seem to estimate the market prices much better than the standard BS model.

4.2.3 Model comparison

For comparative purposes, we will use a measure proposed in [18], which estimates the goodness of fit. It is called root-mean-squared-error (RMSE) and is given by:

$$RMSE = \sqrt{\sum_{i=1}^{N} \frac{(market\ price_i\ -\ model\ price_i)^2}{N}},$$

where N denotes the number of options. Moreover, we also register the computational times because they are an important parameter when comparing models based on numerical methods. Adding to these two measures other features - maxi-

Model	RMSE	max difference	min difference	Computational time(s)
Black Scholes	6.88	25.74	0.098	-
1	1.74	4.5	0.016	2484.25
2	10.93	48.35	0.17	977.85
3	3.62	12.83	0.1	4922.92
4	1.85	4.28	0.039	19231.73

Table 4.2: Comparison between various models

mum and minimum difference between real and estimated prices (in absolute value), Table 4.2 was obtained.

Observing Table 4.2, the measures obtained support what we noticed in the previous section. Comparing the values of the RMSE with the one for the Black-Scholes model, we can see that for the first model it decreases to approximately a quarter of the value, which is consistent with Figure 4.2 (a). Besides that, the minimum and maximum differences are less than what we have for the Black-Scholes, emphasizing that the larger difference for the BS model is more than five times what we have for the first model. For Model 2, as we expected from the Section 4.2.2, the values we get are the worst considering all the models explored in this dissertation. The RMSE is almost twice the value in the BS model as well as the maximum difference between the estimated and the real prices. Model 3 shows an improvement over the Black-Scholes model: the RMSE reduces to approximately half the value of the BS model and the maximum difference between the estimated and market prices also decreases considerably. Between Model 4 and Model 1, there is not much difference: the RMSE is similar for the two models as well as the maximum and minimum differences found among the prices. These two models are the ones with better results.

However, so far we haven't considered the last column of the table, which is important to compare models 1, 3 and 4, the ones that performed better than the standard model. Model 1 takes 2484.25 seconds $\approx$ 41.4 minutes to calibrate the parameters, Model 3 takes 4922.92 seconds $\approx$ 82 minutes $\approx$ 1.37 hours and Model 4 takes 19231.73 seconds $\approx$ 320.53 minutes $\approx$ 5.34 hours (on average). As we can see, Model 4 consumes much more time than the other two models to calibrate the parameters and hence to estimate the option prices. Moreover, Model 1 is the one

that takes less time to calibrate the parameters and combining this with the results observed in Table 4.2, we can conclude that this model is the best among all the models.

To finalize, observing all the results obtained for the local volatility models considered and the comparisons made between them and the original Black-Scholes model, the second one is not a good model because it doesn't estimate the prices better than the standard model. The first, second and fourth models are an improvement over the Black-Scholes, with Model 1 performing better than the others, considering both the numerical results and computational times.

4.3 Prediction

In this section, another property of the models will be studied: we will check if the local volatility models used in the previous section are good predictors, i.e., we will study the ability of the models to predict prices outside sample. The procedure is done in the following way: we calibrate the model considering a certain sub-sample of the data and then predict the prices outside that same sub-sample. Given the conclusions made in the previous sections, we will only perform the described for models 1, 3 and 4.

To study this feature, we distinguish two different sub-samples of the original dataset:

- All strikes from the shorter maturity until 21 July 2017;
- All maturities with strike varying from 2305 to 2395.

These sub-samples were chosen in a way to balance the number of options that will be calibrated and those that will be used for forecasting. We should have more options in the calibration procedure, but we cannot have few in the forecast, otherwise this would affect the purpose of this study.

Replicating the strategy of the previous sections, the values of the parameters (for the two sub-samples) for the models can be found in the Appendix. Comparing the values of the calibration for the whole sample and for each of the sub-samples, we notice that for Model 1 (Table A.2) the first parameters a_0 and a_1 are similar for

all the samples. Looking to the line related to the predictability in time to maturity, the other parameters change significantly, either in magnitude or in sign. In terms of predictability in strike, a_2 is the only parameter that changes in a visible way as it is much bigger than the one calibrated using the entire sample. This suggests that the results for the sub-samples should be different from the ones found on the previous section. For Model 3, in Table A.4, we can see that c_0 is similar along the lines. The second line of the table, related to the predictability in t, shows that all the other parameters change considerably. Looking at the last line, c_1 and d_0 change slightly but c_1 and c_2 are much higher than the parameters calibrated using the complete sample. Like in Model 1, the results for the sub-samples should be different from the ones using the entire sample. For Model 4, the parameters calibrated using each sub-sample are quite different both in magnitude and in sign. With so many differences in the parameters values, we cannot have any idea how the model predicts future prices.

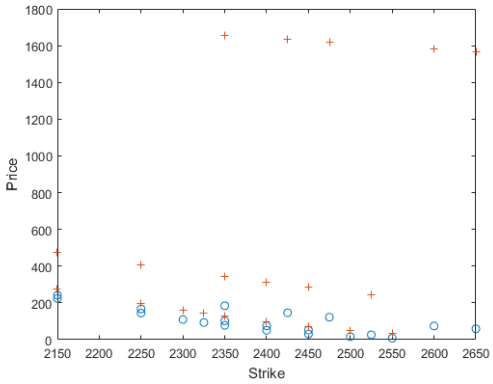

(a) Model 1

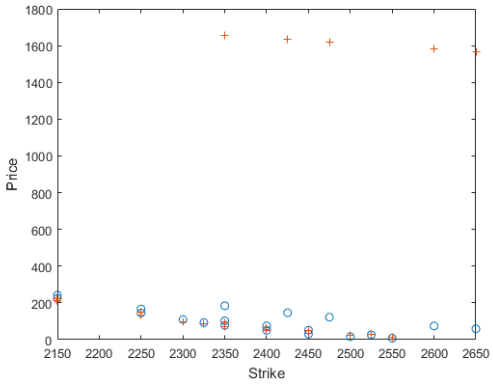

(b) Model 3

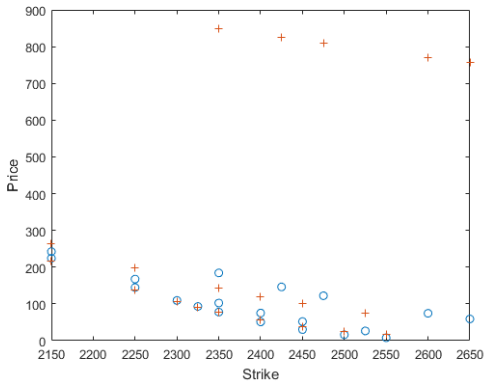

(c) Model 4

Figure 4.4: Predictability in t

Using the values in Tables A.2, A.4 and A.5, two different figures were generated: the first stands for the prediction in time to maturity and the second for the prediction in strike. A table was also generated to show the maximum and minimum differences between real and predicted prices.

Observing Figure 4.4, there is almost no difference between the models. Neither of the models seems to predict well the prices, particularly for the longest time to maturity, where the difference is very impressive. This can also be seen on Table 4.3, where we observe that the maximum differences between the real prices and the predicted ones are 1509.57, 1509.86 and 697.95 for models 1, 3 and 4, respectively.

Looking at Figure 4.5, models 1 and 3 predict the prices in a reasonably way. Still, these models show some discrepancies between estimated and market prices. Model 4 predicts the prices worse than the former models, namely for the longer maturities.

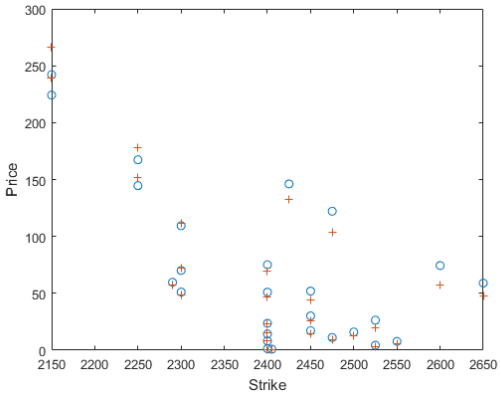

(a) Model 1

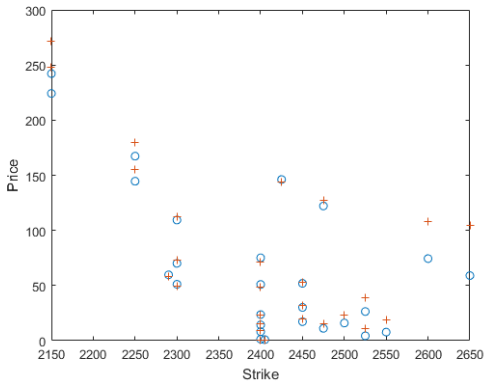

(b) Model 3

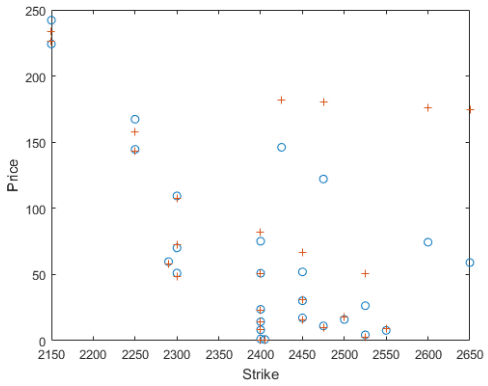

(c) Model 4

Figure 4.5: Predictability in K

Model	Prediction	Max difference	Min difference
1	t	1509.57	25.74
	K	23.74	0.48
3	t	1509.86	0.76
	K	45.54	0.042
4	t	697.95	0.33
	K	115.62	0.12

Table 4.3: Comparison of prediction ability between models 1, 3 and 4

We can conclude that, although these models estimate the prices much better than the Black-Scholes model, their prediction ability is not very good. If we wish to predict the prices with longer times to maturity than those in our sample, they do not seem to find correct values. The same can be said about the prediction of prices with strikes outside the sample, even though the results are better in this case.

Chapter 5

Conclusions

The aim of this dissertation was to improve the famous Black-Scholes model by letting the volatility of the asset price to be a deterministic function of both time and asset price and then study the consequences of this change. Choosing the local volatility to be a parametric function, from a theoretical point of view, does not introduce many changes: the price of an European vanilla call or put option is still explained as the solution of a partial differential equation, derived using the same arguments that Black and Scholes used in their paper. This was possible because this extended model did not add any new source of uncertainty, unlike stochastic volatility models or jump diffusion models. The downside was that the solution of this PDE couldn't be obtained in a closed form, so we needed to use a numerical method: the Crank-Nicolson scheme was the selected one.

Four different functions for the local volatility were formulated and all the parameters involved were calibrated using options on the S&P 500 Index. Numerical results showed that three of these models performed better than Black-Scholes model in estimating the option prices, with Model 1 giving the best results. Regarding the predictive ability, neither of the models performs acceptably in predicting prices with longer time to maturity than the ones in the sample or with strikes outside the sample. This is due to the fact that the calibrated parameters show significant changes from sample to sample.

Bibliography

[1] Black, F. and Scholes, M. (1973). The Pricing of Options and Corporate Liabilities. *Journal of Political Economy* 81 (3), 637-654.

[2] Hull. J. (2012). *Options, Futures and Other Derivatives*, 8th ed. Pearson/Prentice Hall.

[3] Dupire, B. (1994). Pricing with a Smile, *Risk* 7 (1), 18-20.

[4] Daglish T., Hull, J. and Suo, W. (2007). Volatility Surfaces: Theory, Rules of Thumb, and Empirical Evidence. *Quantitative Finance* 7 (5), 507-524.

[5] Dumas, B., Fleming, J. and Whaley, R. (1998). Implied Volatility Functions: Empirical Tests, *The Journal of Finance* 53 (6), 2059-2106.

[6] Brown, G. and Randall, C. (1999). If the skew fits, *Risk*, 62-65.

[7] Lipton, A. (2002). The vol smile problem. *Risk* 15, 61-65.

[8] Derman, E. and Kani, I. (1994). The Volatility Smile and Its Implied Tree. *Quantitative Strategies Research Notes, Goldman Sachs.*

[9] Coleman, T., Li, Y. and Verma, A. (1999). Reconstructing the Unkown Local Volatility Function, *The Journal of Computacional Finance* 2 (3), 77-102.

[10] Merton, R. (1976). Option Pricing when Underlying Stock Returns are Discontinuous. *Journal of Financial Economics* 3 (1-2), 125-144.

[11] Heston, S. (1993). A Closed-Form Solution for Options with Stochastic Volatility with Applications to Bond and Currency Options. *Review of Financial Studies* 6 (2), 327-343.

[12] Hull, J. and White, A. (1987). The Pricing of Options on Assets with Stochastic Volatilities. *The Journal of Finance* 42 (2), 281-300.

[13] Achdou, Y. and Pironneau, O. (2005). *Computational Methods for Option Pricing*. Society for Industrial and Applied Mathematics (SIAM).

[14] Duffy, D. (2006). *Finite Difference Methods in financial engineering*. John Wiley & Sons, Ltd.

[15] Duffy, D. *Robust and Accurate Finite Difference Methods in Option Pricing One Factor Models*. Available from: http://www.datasimfinancial.com/UserFiles/articles/daniel3.pdf

[16] Edwards, D. (2015). *Numerical and Analytical Methods in Option Pricing*. University of Reading. Available from: https://www.overleaf.com/articles/numerical-and-analytic-methods-in-option-pricing/rwpzvzwksgrc/viewer.pdf

[17] White, R. (2013). Numerical Solutions to PDEs with Financial Applications. *OpenGamma Quantitative Research*. Available from: https://developers.opengamma.com/quantitative-research/Numerical-Solutions-to-PDEs-with-Financial-Applications-OpenGamma.pdf

[18] Schoutens, W. (2002). *Lévy Processes in Finance*. Wiley.

[19] Langtangen, H. (2013). *Truncation Error Analysis*. Available from: http://hplgit.github.io/INF5620/doc/pub/main_trunc-A4.pdf

[20] Eriksson, A. (2013). *A comparison between finite difference and binomial methods for solving American single-stock options*. Master Thesis. Royal Institute of Technology.

[21] Tavella, D. and Randall, C. (2000). *Pricing Financial Instruments: The Finite Difference Method*. John Wiley & Sons, Inc.

[22] Campolieti, G. and Makarov, R. (2014). *Financial Mathematics: A comprehensive treatment*. Chapman & Hall/CRC.

[23] Rubinstein, M. (1994). Implied Binomial Trees. *The Journal of Finance* 49 (3), 771-818.

[24] Vidic, I. (2012). *Numerical methods for option pricing.* Master Thesis. Politecnica de Madrid.

[25] Chan, R. (2016). *Chapter 9: Numerical Methods for Option Pricing*, MAT4210 Notes. Available from: https://www.math.cuhk.edu.hk/course_builder/1617/math4210/ [28 July 2017].

[26] Kuan, C. (2014). *Chapter 8: Nonlinear Least Squares Theory*, Lectures. Available from: http://homepage.ntu.edu.tw/~ckuan/e-courses.html [28 July 2017].

[27] Mukherji, S. (2011). The Capital Asset Pricing Model's Risk-free Rate. *The International Journal of Business and Finance Research* 5 (2), 75-83.

[28] U.S. Department of the Treasury. Available from: https://www.treasury.gov/resource-center/data-chart-center/interest-rates/Pages/TextView.aspx?data=billRatesYear&year=2017 [6 July 2017].

[29] MatLab Documentation. Available from: https://www.mathworks.com/help/curvefit/least-squares-fitting.html [30 March 2017].

Appendix A

Numerical Code, Data and Parameter Values

A.1 C-N method code

```
%N - number of time intervals
%M - number of space intervals
%(xmin,xmax) - domain of the space variable
%T - final time
%initial - intial condition: t=0
%down - boundary condition at xmin
%up - boundary condition at xmax
%a,b,c,f - coefficients of the PDE: a*uxx+b*ux+c*u-ut=0 as functions. It
%should be passed as strings: 'a', 'b', 'c' and 'f' or @a, etc...

function [t,x,u]=CrankN_fit(param,xdata,initial,down,up,a,b,c,f,S0,r)
N=xdata(1);
M=xdata(2);
xmin=xdata(3);
xmax=xdata(4);
T=xdata(5);
%create the grid in time and space
```

```
%in time: divide [0,T] into N intervals
k=T/N; %time step
t=0:k:T; %t(n)=(n-1)*k, n=1,...,N+1
%in space: divide [xmin,xman] into M intervals
h=(xmax-xmin)/M; %space step
x=xmin:h:xmax; %x(i)=xmin+(i-1)*h, i=1,...,M+1
u=zeros(M+1,N+1); %matrix where the solutions will be put
%set initial condition
for i=1:(M+1)
    u(i,1)=feval(initial,S0,x(i));
end
%initialize method
for j=2:N+1
    F=zeros(M+1); %matrix used to get solutions in the next time step
    D=zeros(M+1,1);
    F(1,1)=1; %to get boundary conditions in the matrix form
    F(M+1,M+1)=1;
    %set boundary conditions
    D(1,1)=feval(down,S0,t(j))
    D(M+1,1)=feval(up,t(j));
    for i=2:M
        a_actual=feval(a,param,S0,x(i),t(j-1)); %functions at current time
        b_actual=feval(b,r,x(i),t(j-1));
        c_actual=feval(c,x(i),t(j-1));
        a_next=feval(a,param,S0,x(i),t(j)); %functions at next time
        b_next=feval(b,r,x(i),t(j));
        c_next=feval(c,x(i),t(j));
        f_actual=feval(f,x(i),0.5*(t(j)+t(j-1))); %f at time t+1/2
        %set elements of the matrix
        F(i,i-1)=2*k*a_next-h*k*b_next;
        F(i,i)=-4*h^2-4*k*a_next+2*h^2*k*c_next;
        F(i,i+1)=2*k*a_next+h*k*b_next;
```

```
        D(i,1)=-u(i+1,j-1)*(2*k*a_actual+h*k*b_actual)-u(i,j-1)*(4*h^2
        -4*k*a_actual+2*h^2*k*c_actual)-u(i-1,j-1)*(2*k*a_actual
        -h*k*b_actual)+4*h^2*k*f_actual;
    end
    u(:,j)=linsolve(F,D); %solve system to get values at next time step
end
end
```

A.2 Data

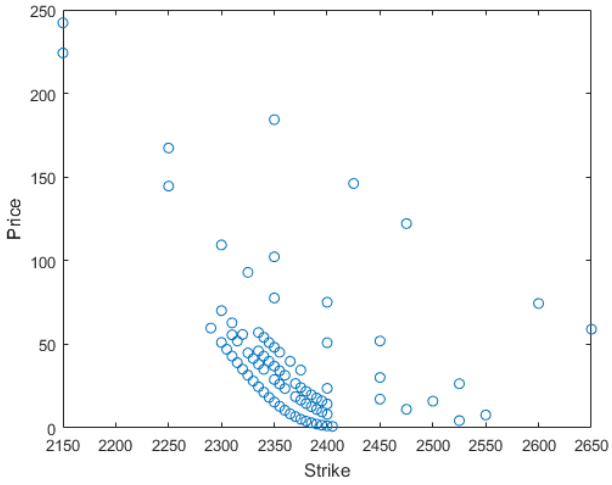

Figure A.1: Call option prices against Strike

Strike	31 March 2017	28 April 2017	19 May 2017	16 June 2017	21 July 2017	15 September 2017	15 December 2017	21 December 2018
2150						224.2	242.2	
2250						144.6	167.3	
2290	59.7							
2300	51.1		70.1			109.4		
2305	47							
2310	42.95	55.7	62.8					
2315	39	51.95						
2320	35.1		55.9					
2325	31.5	44.9				93		
2330	28	41.5						
2335	24.6	38.1	45.99	57.05				
2340	21.3	35	43	54.2				
2345	18.3		39.8	51.05				
2350	15.5	28.9	36.95	48.2		77.7	102.3	184.3
2355	12.9	26.2	34.2	45.3				
2360	10.6	23.5	31.5					
2365	8.4			39.8				
2370	6.8	18.7	26.5					
2375	5.2	16.6	24.2	34.6				
2380	4.05	14.6	21.9					
2385	3.1	12.7	19.8					
2390	2.3	11.1	17.9					
2395	1.7	9.5	16.1					
2400	1.3	8.2	14.3	23.6		50.9	75.2	
2405	0.9							
2425								146.2
2450					17.2	30.2	51.9	
2475					11.2			122.1
2500						16		
2525					4.3		26.4	
2550						7.8		
2600								74.4
2650								59

Table A.1: Call options

A.3 Parameter values

Parameters	a_0	a_1	a_2	a_3	a_4	a_5
Whole sample	0.1002	-0.7272	1.3017	0.0659	-0.0224	0.2630
Predictability in t	0.1201	-1.1021	3.8869	-0.4346	2.0190	-1.2028
Predictability in K	0.1013	-1.1731	8.2046	0.0423	-0.0166	-0.0039

Table A.2: Calibrated parameters for volatility function 1

Parameters	b_0	b_1	b_2	b_3
Whole sample	0.09905	-0.0001	1.0e-07×-8.96	1.0e-10×2.11

Table A.3: Calibrated parameters for volatility function 2

Parameters	c_0	c_1	c_2	c_3	d_0
Whole sample	0.1079	-0.5984	7.9975	-5.7968	-0.0808
Predictability in t	0.1076	0.8529	1.8210	-0.0000	-44.4086
Predictability in K	0.0931	-0.9319	19.8466	-9.7225	0.1012

Table A.4: Calibrated parameters for volatility function 3

Parameters		Whole sample	Predictability in t	Predictability in K
σ_{ATM}	β_1	129788.69	11160.36	4.54
	β_2	2013.31	18234.66	0.78
	β_3	259177.4	22094.03	-0.027
σ_{skew}	α_1	91.36	17973.97	3.99
	α_2	-6.41	-6774.49	0.69
	α_3	191.6	11911.95	-0.14
λ_{skew}	γ_1	0.55	-17.64	-6.52
	γ_2	-0.23	-6.25	14.17
	γ_3	-1.11	261.66	-0.21
θ_{skew}	θ_1	-23.36	2094.47	11.61
	θ_2	0.047	6807.04	-0.46
	θ_3	-20.21	7906.1	4.15

Table A.5: Calibrated parameters for volatility function 4